

Van der Waals density functional: Self-consistent potential and the nature of the van der Waals bond

T. Thonhauser,¹ Valentino R. Cooper,¹ Shen Li,¹ Aaron Puzder,¹ Per Hyldgaard,² and David C. Langreth¹

¹*Department of Physics and Astronomy, Rutgers,
The State University of New Jersey, Piscataway, New Jersey 08854-8019, USA.*

²*Department of Microtechnology and Nanoscience,
Chalmers University of Technology, SE-412 96 Göteborg, Sweden.*

(Dated: September 14, 2018)

We derive the exchange-correlation potential corresponding to the nonlocal van der Waals density functional [M. Dion, H. Rydberg, E. Schröder, D. C. Langreth, and B. I. Lundqvist, *Phys. Rev. Lett.* **92**, 246401 (2004)]. We use this potential for a self-consistent calculation of the ground state properties of a number of van der Waals complexes as well as crystalline silicon. For the latter, where little or no van der Waals interaction is expected, we find that the results are mostly determined by semilocal exchange and correlation as in standard generalized gradient approximations (GGA), with the fully nonlocal term giving little effect. On the other hand, our results for the van der Waals complexes show that the self-consistency has little effect at equilibrium separations. This finding validates previous calculations with the same functional that treated the fully nonlocal term as a post GGA perturbation. A comparison of our results with wave-function calculations demonstrates the usefulness of our approach. The exchange-correlation potential also allows us to calculate Hellmann-Feynman forces, hence providing the means for efficient geometry relaxations as well as unleashing the potential use of other standard techniques that depend on the self-consistent charge distribution. The nature of the van der Waals bond is discussed in terms of the self-consistent bonding charge.

PACS numbers: 31.15.Ew, 71.15.Mb, 61.50.Lt

I. INTRODUCTION

Density functional theory (DFT) has acquired high respect for its simplicity and accuracy within first-principles calculations. In particular, generalized gradient approximations^{1,2,3} have had much success in describing isolated molecules⁴ as well as dense bulk matter.⁵ For molecules, this performance has been further improved by the use of various empirical and hybrid methods. On the other hand, for van der Waals (vdW) complexes and sparse matter, including many layered structures, polymer crystals, and organic molecular crystals, these methods either give sporadic results or fail completely. The reason for this failure is that the dominant part of the stabilization energy in many cases comes from the dispersion energy, which is not correctly accounted for in standard DFT.^{6,7,8,9,10}

To remedy the situation, a new approach using a van der Waals density functional (vdW-DF) with a nonlocal correlation energy has been developed.¹⁰ This formalism includes van der Waals forces in a seamless fashion and has been applied with quite good results to bulk layered systems,⁹ dimers,^{10,11,12,13,14,15,16} molecules physisorbed on infinite surfaces,¹⁷ and bulk crystals of polyethylene.¹⁸ Lacking the exchange-correlation potential corresponding to the vdW-DF, these calculations evaluated the vdW-DF as a post-processing perturbation, using a charge density obtained from self-consistent calculations with the PBE or revPBE functionals.^{2,3}

The goal of this paper is to derive the exchange-correlation potential for the vdW-DF, thereby enabling fully self-consistent calculations using vdW-DF. This

exchange-correlation potential will give more credibility to the post-process vdW-DF calculations mentioned above. Furthermore, it encourages us to apply the vdW-DF to even more exciting cases in the future. In addition, the knowledge and implementation of the exchange-correlation potential provides the missing underlying framework for further developments, such as the evaluation of forces and the stress tensor. These tools are of tremendous interest for the structural optimization of many soft materials. Also many other standard tools for analyzing materials properties that are usually built into ab-initio codes become accessible through the self-consistent vdW-DF potential. With these developments, vdW-DF should become a standard tool for systems where vdW interactions are important. This includes not only extended systems, but also finite systems that are too large for the standard quantum chemical methods to be effective.

For such large finite systems, the advantage of the vdW-DF approach becomes obvious when the scaling of the computational effort with respect to system size is considered. Particular interest in van der Waals complexes has emerged in the context of large systems, where questions regarding DNA base-pair bonding, protein structure and folding, and organic molecule crystallization are experiencing a surge of interest. Traditionally, second-order Møller-Plesset perturbation theory¹⁹ (MP2) and coupled-cluster calculations²⁰ with singles, doubles, and perturbative triple excitations (CCSD(T)) would be used to study these systems as they are regarded as accurate and reliable. Unfortunately, in many of these cases their application is limited to relatively

small systems, since they are too computationally demanding. Furthermore, the results are basis set dependent and elaborate techniques are necessary to estimate results at the complete basis set limit. This is where the strength of the vdW-DF approach lies: Since it scales with system size N just like a regular DFT calculation—usually $\mathcal{O}(N^3)$, complexes currently out of the reach for MP2 and CCSD(T) calculations are easily treatable.

For extended systems that require the consideration of long-range van der Waals interactions, the advantage of vdW-DF is even more obvious. To our knowledge there is simply no other first-principles method available. The earlier post-process application of the method has already given reasonable results for a polymer crystal¹⁸ and layered intercalates,²¹ and applications to molecular crystals are under way. The results of this work suggest that the predictions will not be greatly affected by the full self-consistency that now becomes possible.

The vdW-DF treats the nonlocal vdW interaction by an approximate non-empirical method that is not only correct in principle, but useful in practice. It differs from other methods^{22,23,24,25,26,27,28,29} that treat the vdW interaction as occurring directly between the nuclei via empirically determined potentials. As discussed later, the correct source for the forces on the nuclei is electrostatic, and results from a change in the charge densities of the fragments as the vdW bond is formed. This effect is included correctly in vdW-DF.

We have organized this paper in the following way. In Sec. II we analytically derive the exchange-correlation potential. In Sec. III the potential is then applied to several, very different physical systems. We compare our results with other calculations such as MP2 and CCSD(T) and find good agreement. Our results show that calculating vdW-DF binding energies in a post-process procedure, rather than self-consistent, is reasonable, thus justifying the approximation used in earlier calculations. Here, we also deal with the question of how the vdW-DF performs for solids and covalently bonded systems such as a CO₂ molecule or crystalline Si. In Sec. IV we use the vdW-DF self-consistent charge density to discuss the nature of the van der Waals bond. We conclude in Sec. V. Some details of the derivation of the potential are collected in Appendices A, B, and C.

II. DERIVATION OF THE EXCHANGE-CORRELATION POTENTIAL

The density functional in question is defined in Ref. [10]. It consists of several different contributions, i.e.

$$E_{xc}[n] = E_x^{\text{revPBE}}[n] + E_c^{\text{LDA}}[n] + E_c^{\text{nl}}[n]. \quad (1)$$

The first two parts are simply revPBE exchange and LDA correlation. We note that these parts represent LDA plus gradient corrections and are hence *semilocal*. The van der

Waals interaction enters through a fully *nonlocal* correction $E_c^{\text{nl}}[n]$ that concerns the correlation only. In the following we are interested in the exchange-correlation potential that originates from this nonlocal contribution. However, we have to keep in mind that the total exchange-correlation potential corresponding to Eq. (1) also includes the parts stemming from $E_x^{\text{revPBE}}[n]$ and $E_c^{\text{LDA}}[n]$ —these expressions are well-known and can be found elsewhere.^{30,31}

In order to calculate the potential of interest, we have to take the functional derivative of the energy with respect to the density, i.e.

$$E_c^{\text{nl}}[n] = \frac{1}{2} \int d^3r d^3r' n(\mathbf{r}) \phi(\mathbf{r}, \mathbf{r}') n(\mathbf{r}'), \quad (2)$$

$$v_c^{\text{nl}}(\tilde{\mathbf{r}}) = \frac{\delta E_c^{\text{nl}}[n]}{\delta n(\tilde{\mathbf{r}})}, \quad (3)$$

where $\phi(\mathbf{r}, \mathbf{r}')$ is a function depending on $\mathbf{r} - \mathbf{r}'$ and the electronic densities n and the magnitude of their gradients at the points \mathbf{r} and \mathbf{r}' . Details about the kernel $\phi(\mathbf{r}, \mathbf{r}')$ and its evaluation can be found in Appendix A. It follows that

$$\begin{aligned} v_c^{\text{nl}}(\tilde{\mathbf{r}}) &= \frac{1}{2} \int d^3r d^3r' \frac{\delta n(\mathbf{r})}{\delta n(\tilde{\mathbf{r}})} \phi(\mathbf{r}, \mathbf{r}') n(\mathbf{r}') \\ &+ \frac{1}{2} \int d^3r d^3r' n(\mathbf{r}) \phi(\mathbf{r}, \mathbf{r}') \frac{\delta n(\mathbf{r}')}{\delta n(\tilde{\mathbf{r}})} \\ &+ \frac{1}{2} \int d^3r d^3r' n(\mathbf{r}) \frac{\delta \phi(\mathbf{r}, \mathbf{r}')}{\delta n(\tilde{\mathbf{r}})} n(\mathbf{r}'). \end{aligned} \quad (4)$$

The first two lines can be simplified if we use

$$\frac{\delta n(\mathbf{r})}{\delta n(\tilde{\mathbf{r}})} = \delta(\mathbf{r} - \tilde{\mathbf{r}}). \quad (5)$$

It turns out that the kernel $\phi(\mathbf{r}, \mathbf{r}')$ depends on \mathbf{r} and \mathbf{r}' only through two functions d and d'

$$d(\mathbf{r}, \mathbf{r}') = |\mathbf{r} - \mathbf{r}'| q_0(\mathbf{r}) = R_{\mathbf{r}\mathbf{r}'} q_0(\mathbf{r}) \quad (6a)$$

$$d'(\mathbf{r}, \mathbf{r}') = |\mathbf{r} - \mathbf{r}'| q_0(\mathbf{r}') = R_{\mathbf{r}\mathbf{r}'} q_0(\mathbf{r}'), \quad (6b)$$

where we have introduced $\mathbf{R}_{\mathbf{r}\mathbf{r}'} = \mathbf{r} - \mathbf{r}'$ and $R_{\mathbf{r}\mathbf{r}'} = |\mathbf{R}_{\mathbf{r}\mathbf{r}'}|$. The definition of $q_0(\mathbf{r})$ can be found in Eqs. (11) and (12) of Ref. [10] which reads

$$q_0(\mathbf{r}) = -\frac{4\pi}{3} \varepsilon_{xc}^{\text{LDA}} n(\mathbf{r}) - \frac{Z_{ab}}{9} s^2(\mathbf{r}) k_{\text{F}}(\mathbf{r}), \quad (7)$$

where we have used the standard expressions for the Fermi wave vector and the reduced gradient

$$k_{\text{F}}^3(\mathbf{r}) = 3\pi^2 n(\mathbf{r}), \quad \mathbf{s}(\mathbf{r}) = \frac{\nabla n(\mathbf{r})}{2k_{\text{F}}(\mathbf{r}) n(\mathbf{r})}, \quad (8)$$

and $Z_{ab} = -0.8491$. A complete discussion of the gradient term in Eq. (7) is given in Appendix B.

We may now write

$$\phi(\mathbf{r}, \mathbf{r}') = \phi(d(\mathbf{r}, \mathbf{r}'), d'(\mathbf{r}, \mathbf{r}')) = \phi(d, d') = \phi(d', d). \quad (9)$$

The symmetry in the last equality is apparent by exploiting the definition of $\phi(\mathbf{r}, \mathbf{r}')$ in Appendix A. In order to calculate the derivative in the third line of Eq. (4) we can use this symmetry and find

$$\frac{\delta\phi(\mathbf{r}, \mathbf{r}')}{\delta n(\tilde{\mathbf{r}})} = \frac{\partial\phi(d, d')}{\partial d} \frac{\delta d}{\delta n(\tilde{\mathbf{r}})} + \frac{\overbrace{\partial\phi(d, d')}^{\phi(d', d)}}{\partial d'} \frac{\delta d'}{\delta n(\tilde{\mathbf{r}})}. \quad (10)$$

If we keep in mind that both terms appear under a double integral, we can change the integration variables and find that these two terms are equivalent. Then, simply inserting a factor of two and abbreviating $\frac{\partial\phi(d, d')}{\partial d} = \phi_d(d, d') = \phi_d(\mathbf{r}, \mathbf{r}')$ yields

$$v_c^{\text{nl}}(\tilde{\mathbf{r}}) = \int d^3r' \phi(\tilde{\mathbf{r}}, \mathbf{r}') n(\mathbf{r}') \quad (11)$$

$$+ \int d^3r d^3r' n(\mathbf{r}) \phi_d(\mathbf{r}, \mathbf{r}') \frac{\delta d(\mathbf{r}, \mathbf{r}')}{\delta n(\tilde{\mathbf{r}})} n(\mathbf{r}').$$

The missing derivative in the equation above follows from the definition of $d(\mathbf{r}, \mathbf{r}')$ in Eq. (6), i.e.

$$\frac{\delta d(\mathbf{r}, \mathbf{r}')}{\delta n(\tilde{\mathbf{r}})} = R_{\mathbf{r}\mathbf{r}'} \frac{\delta q_0(\mathbf{r})}{\delta n(\tilde{\mathbf{r}})}. \quad (12)$$

If we denote the derivative of $\varepsilon_{\text{xc}}^{\text{LDA}}$ with respect to the density as $\varepsilon_{\text{xc}}^{\text{LDA}'}$ and simplify further, it follows

$$\frac{\delta q_0(\mathbf{r})}{\delta n(\tilde{\mathbf{r}})} = -\frac{4\pi}{3} \varepsilon_{\text{xc}}^{\text{LDA}'(\mathbf{r})} \delta(\mathbf{r} - \tilde{\mathbf{r}}) \quad (13)$$

$$- \frac{Z_{ab}}{9} \frac{1}{n(\mathbf{r})} \mathbf{s}(\mathbf{r}) \cdot \nabla \delta(\mathbf{r} - \tilde{\mathbf{r}})$$

$$+ \frac{7}{3} \frac{Z_{ab}}{9} \frac{1}{n(\mathbf{r})} s^2(\mathbf{r}) k_{\text{F}}(\mathbf{r}) \delta(\mathbf{r} - \tilde{\mathbf{r}}).$$

Equation (13) together with Eq. (12) can now be inserted in the expression for the potential, Eq. (11), and it follows

$$v_c^{\text{nl}}(\tilde{\mathbf{r}}) = \int d^3r' \phi(\tilde{\mathbf{r}}, \mathbf{r}') n(\mathbf{r}') \quad (14)$$

$$- \frac{4\pi}{3} \int d^3r' n(\tilde{\mathbf{r}}) \phi_d(\tilde{\mathbf{r}}, \mathbf{r}') R_{\tilde{\mathbf{r}}\mathbf{r}'} \varepsilon_{\text{xc}}^{\text{LDA}'(\tilde{\mathbf{r}})} n(\mathbf{r}')$$

$$- \frac{Z_{ab}}{9} \int d^3r d^3r' \phi_d(\mathbf{r}, \mathbf{r}') R_{\mathbf{r}\mathbf{r}'} \mathbf{s}(\mathbf{r}) \cdot (\nabla \delta(\mathbf{r} - \tilde{\mathbf{r}})) n(\mathbf{r}')$$

$$+ \frac{7}{3} \frac{Z_{ab}}{9} \int d^3r' \phi_d(\tilde{\mathbf{r}}, \mathbf{r}') R_{\tilde{\mathbf{r}}\mathbf{r}'} s^2(\tilde{\mathbf{r}}) k_{\text{F}}(\tilde{\mathbf{r}}) n(\mathbf{r}').$$

The third line in this equation includes the gradient of the δ -function. Partial integration lets us rewrite the corresponding integral as

$$+ \frac{Z_{ab}}{9} \int d^3r' \nabla_{\tilde{\mathbf{r}}} \cdot [\phi_d(\tilde{\mathbf{r}}, \mathbf{r}') R_{\tilde{\mathbf{r}}\mathbf{r}'} \mathbf{s}(\tilde{\mathbf{r}})] n(\mathbf{r}'),$$

where the sufficiently rapid fall-off of ϕ_d (see Eq. 20) guarantees the vanishing of the integrated part. All contributions now have the common form $\int d^3r' \dots n(\mathbf{r}')$ so that,

after dropping the tilde ($\tilde{\mathbf{r}} \rightarrow \mathbf{r}$), we may simply write:

$$v_c^{\text{nl}}(\mathbf{r}) = \int d^3r' n(\mathbf{r}') \times \quad (15)$$

$$\left[\phi(\mathbf{r}, \mathbf{r}') + \frac{Z_{ab}}{9} \nabla \cdot [\phi_d(\mathbf{r}, \mathbf{r}') R_{\mathbf{r}\mathbf{r}'} \mathbf{s}(\mathbf{r})] \right.$$

$$\left. + \phi_d(\mathbf{r}, \mathbf{r}') R_{\mathbf{r}\mathbf{r}'} \left(\frac{7}{3} \frac{Z_{ab}}{9} s^2(\mathbf{r}) k_{\text{F}}(\mathbf{r}) - \frac{4\pi}{3} n(\mathbf{r}) \varepsilon_{\text{xc}}^{\text{LDA}'(\mathbf{r})} \right) \right].$$

The term including the gradient $\nabla \cdot [\dots]$ in the equation above can be further simplified, but the details are deferred to Appendix C. If we use Eq. (6) to replace $R_{\mathbf{r}\mathbf{r}'}$ in favor of $d(\mathbf{r}, \mathbf{r}')$ or $d'(\mathbf{r}, \mathbf{r}')$ and collect similar terms, we find as the final result

$$v_c^{\text{nl}}(\mathbf{r}) = \int d^3r' n(\mathbf{r}') \sum_{i=1}^4 \alpha_i(\mathbf{r}, \mathbf{r}') \Phi_i(\mathbf{r}, \mathbf{r}'), \quad (16)$$

where the functions $\alpha_i(\mathbf{r}, \mathbf{r}')$ and $\Phi_i(\mathbf{r}, \mathbf{r}')$ are given by:

$$\alpha_1 = \frac{1}{q_0(\mathbf{r})} \left[\frac{Z_{ab}}{9} \nabla \cdot \mathbf{s}(\mathbf{r}) + \frac{7}{3} \frac{Z_{ab}}{9} s^2(\mathbf{r}) k_{\text{F}}(\mathbf{r}) \right. \quad (17a)$$

$$\left. - \frac{4\pi}{3} n(\mathbf{r}) \varepsilon_{\text{xc}}^{\text{LDA}'(\mathbf{r})} \right]$$

$$\alpha_2 = \frac{Z_{ab} \mathbf{s}(\mathbf{r}) \cdot \nabla q_0(\mathbf{r})}{9 q_0(\mathbf{r})^2} \quad (17b)$$

$$\alpha_3 = \frac{Z_{ab}}{9} \hat{\mathbf{R}}_{\mathbf{r}\mathbf{r}'} \cdot \mathbf{s}(\mathbf{r}) \quad (17c)$$

$$\alpha_4 = 1 \quad (17d)$$

and

$$\Phi_1 = d\phi_d(d, d') \quad (18a)$$

$$\Phi_2 = d^2\phi_{dd}(d, d') \quad (18b)$$

$$\Phi_3 = \phi_d(d, d') + d\phi_{dd}(d, d') + d'\phi_{dd'}(d, d') \quad (18c)$$

$$\Phi_4 = \phi(d, d'), \quad (18d)$$

where Φ_4 is the kernel function defined in Ref. [10]. Here, we have abbreviated higher order derivatives of $\phi(d, d')$ as previously,

$$\frac{\partial^2 \phi(d, d')}{\partial d \partial d} = \phi_{dd}(d, d') \quad \text{and} \quad \frac{\partial^2 \phi(d, d')}{\partial d \partial d'} = \phi_{dd'}(d, d').$$

For completeness, details about the evaluation of $\phi_d(d, d')$, $\phi_{dd}(d, d')$, and $\phi_{dd'}(d, d')$ are provided in Appendix A.

The three extra internal kernel functions $\Phi_1(d, d')$ through $\Phi_3(d, d')$ in Eqs. (18a–18c) necessary for v_c^{nl} are the analogues of the single function $\phi(d, d')$ ($\equiv \Phi_4(d, d')$) used for E_c^{nl} . However, unlike the latter, they are not symmetric under the exchange of d and d' . Consequently, when expressed in terms of the sum and difference variables D and δ defined by¹⁰

$$d = D(1 + \delta), \quad (19a)$$

$$d' = D(1 - \delta), \quad (19b)$$

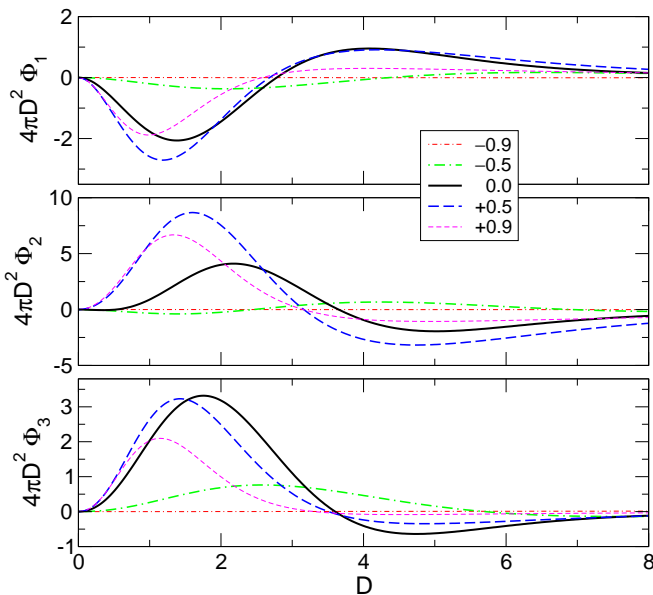


FIG. 1: The kernels Φ_1 , Φ_2 , and Φ_3 given in Eqs. (18) are plotted as a function of D for values of $\delta = \pm 0.9, \pm 0.5$, and 0.0 [see Eqs. (19)].

their values depend on the sign of δ . Plots of these three new kernels are given in Fig. 1. Comparison with Fig. 1 of Ref. [10] (see erratum), shows that there are no unexpected features. The details of the evaluation are given in Appendix A. The asymptotic form of the kernels for v_c^{nl} for large $R \equiv |\mathbf{r} - \mathbf{r}'|$ may be determined by using the relation¹⁰

$$\phi(d, d') \rightarrow -\frac{12(4\pi/9)^3}{d^2 d'^2 (d^2 + d'^2)}. \quad (20)$$

The use of Eq. (20) in Eqs. (18) plus the fact that $D \propto R^1$ and $\delta \propto R^0$ gives the asymptotic dependence R^{-6} to Φ_1 , Φ_2 , and Φ_4 , while Φ_3 falls off faster and thus does not contribute to the asymptote.

The asymptotic form above follows from the form of the model response function that determines the kernels. It gives the correct asymptotic dependence for all finite sized fragments, and for all infinite fragments that are not metallic. A couple of decades ago, Barash³² showed that infinite metallic fragments of reduced dimensionality could show a more slowly decaying asymptote than would be given by the appropriate integrals over (20). This effect occurs because the dipole response functions of infinite metals may not be sufficiently convergent at small frequency and wave vector. A number of examples of special cases have been worked out more recently.³³ We can say with certainty that, with the response function presently used, our functional will fail for infinite metallic (or semimetallic) fragments of reduced dimensionality at very large distances (for example, parallel metallic sheets). The distance where the crossover occurs will depend on the details of the material. We are unaware of any such material where this distance is known.

The arrangement of the results for v_c^{nl} in Eq. (16) according to Eqs. (17) and (18) was chosen to facilitate rapid numerical evaluation. For a grid of N points, the evaluation of v_c^{nl} on each is $\mathcal{O}(N^2)$ according to Eq. (16). However, the evaluation of the Φ 's in Eqs. (18) needs only to be done once to create an interpolation table. The conversion between \mathbf{r} (\mathbf{r}') and d (d') [Eqs. (6)] of course needs to be done $\mathcal{O}(N^2)$ times, but the lengthy part of that would be the calculation of q_0 , which instead can be calculated in advance on each grid point, i.e. it is $\mathcal{O}(N)$. The calculation of α_1 and α_2 [Eqs. (17)] is $\mathcal{O}(N)$. So, the only parts of the calculation that are $\mathcal{O}(N^2)$ are the calculation of the components of \mathbf{R} for α_3 [Eq. (17c)], the calculation of $|\mathbf{R}|$ for \mathbf{r} to d conversion [Eqs. (6)], two table interpolations, and a few arithmetic operations.

III. RESULTS

The exchange-correlation potential derived in the previous section will now be applied to various systems. Calculations labeled as self-consistent (SC) include the potential (3) as part of the Kohn-Sham potential, so that the density used to evaluate the nonlocal correlation energy, Eq. (2), is fully self-consistent. Results in which the nonlocal vdW correlation energy (2) is calculated using the density from a self-consistent PBE calculation will be referred to as non-SC. It should be noted that all previous vdW-DF calculations^{9,10,11,12,13,14,15,16,17,18} were performed with such a non-SC post-process procedure.

It is apparent that the post-process evaluation of the vdW-DF is an approximation since the charge density is not allowed to evolve under the full vdW-DF functional. Although there are many arguments that the effect of this approximation is small, the ultimate test is obviously a comparison of our new SC results with the older non-SC results. In the following we shall make this comparison.

In addition to the SC and non-SC results, we will also show results marked as “no E_c^{nl} ”. These results were obtained by only considering $E_x^{\text{revPBE}} + E_c^{\text{LDA}}$ in Eq. (1) and neglecting the nonlocal part E_c^{nl} . This will allow us to prove that the correct behavior of the vdW-DF for van der Waals systems indeed is encoded in the nonlocal correlation E_c^{nl} . The calculations below were made with the aid of the plane-wave code ABINIT³⁴ and the real-space code PARSEC.³⁵

A. Ar and Kr dimers

We start out by applying the self-consistent vdW-DF to some rare gas dimers, which, due to their closed valence shells, owe much of their binding to van der Waals interactions. Results for the interaction energy of an Ar and a Kr dimer as a function of separation are depicted in Figs. 2 and 3. It can be seen that the differences between SC and non-SC calculations are indeed very small, and

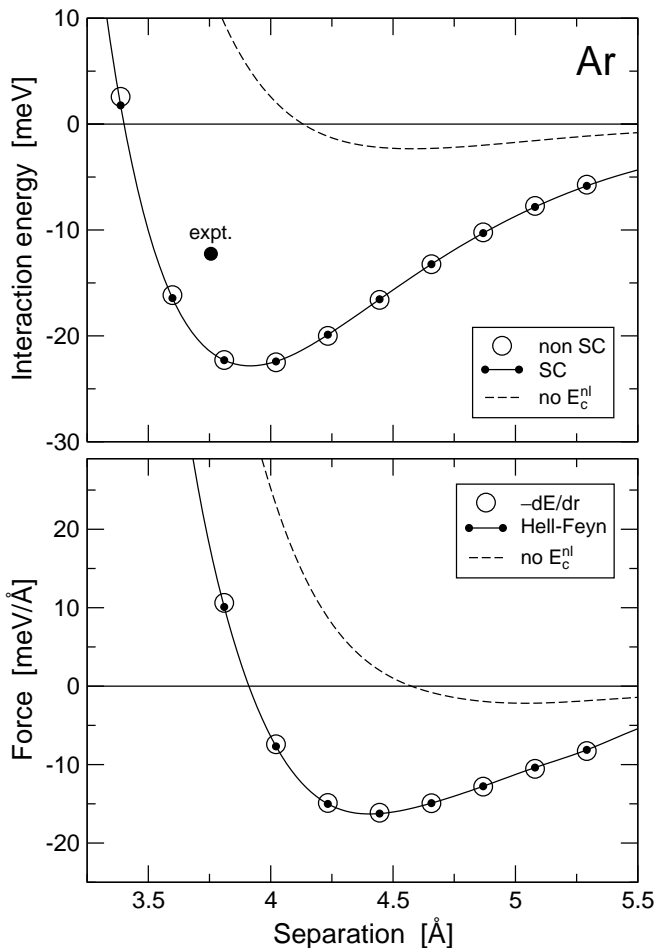


FIG. 2: **(top)** Interaction energy of the Ar dimer as a function of separation. Plotted are self-consistent and non self-consistent results. In addition, we show results where E_c^{nl} has been neglected. Experimental values are taken from Ref. [36]. **(bottom)** Forces calculated as the derivative of the energy ($-dE/dr$) and the Hellmann-Feynman forces.

on the scale of this plot they are negligible. In general, these differences are larger for smaller separations, where the perturbation from the nonlocal term is larger. For Ar and Kr we find the binding distances to be 3.9 Å and 4.2 Å, which is approximately 5% larger than their corresponding experimental values.³⁶ On the other hand, our interaction energies are stronger than experiment. This behavior of the binding distance is consistent with all previous calculations^{9,10,11,12,13,14,15,16,17,18} and has been attributed to the form of the exchange used.^{12,13} In addition, it can be seen that without the nonlocal contribution (no E_c^{nl}) the binding is much too weak and the separation is too large. In some cases, as we shall see later in the text, without this contribution binding does not occur at all. It thus becomes obvious that the addition of the nonlocal contribution E_c^{nl} dramatically improves the description of these van der Waals systems.

As a result of our DFT calculations, we not only obtain the energies discussed above, but also the correspond-

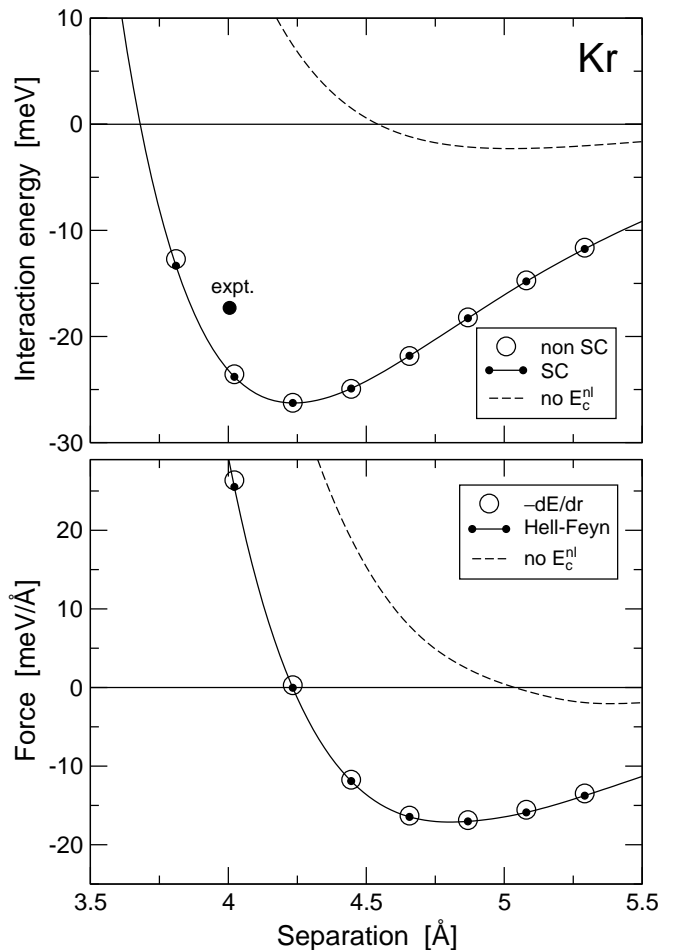


FIG. 3: Same as Fig. 2 except here describing the Kr dimer.

ing Hellmann-Feynman forces which act on each nuclei. These are simply the electrostatic forces, which require the correct self-consistent charge distribution for their determination. Until now, it was impossible to obtain them within vdW-DF. Results for these forces are plotted in the bottom panels of Figs. 2 and 3. In order to verify the correctness of these forces, we have plotted the negative derivative of the energy from above ($-dE/dr$). It can be seen that the zero point of the forces perfectly aligns with the corresponding energy minimum. As for the energy, we have again included results for “no E_c^{nl} ”. It is now apparent that semilocal exchange-correlation alone cannot describe van der Waals systems correctly and most of the binding force originates in the nonlocal part of the functional.

B. CO₂ dimer

Next, we apply the vdW-DF to a slightly more complex molecule, i.e. the CO₂ dimer. However, before we discuss the details about the dimer, it is interesting to first explore the behavior of the vdW-DF for a single

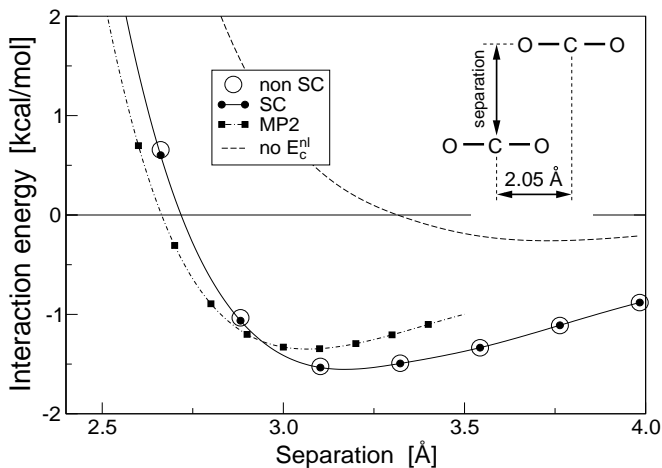


FIG. 4: Interaction energy of a CO₂ dimer as a function of its separation at a fixed slip distance of 2.05 Å. The inset shows the CO₂ dimer geometry.

CO₂ molecule. The CO₂ molecule is a covalently bonded system, with only minor contributions from vdW interactions. As such, it is interesting to investigate how vdW-DF treats such a system. The important question here is whether or not the functional will continue to give good results for cases in which van der Waals interactions are negligible or non-existent.

For CO₂ we can partly answer this question by calculating the optimal C–O bond length. Our results show that the bond length that vdW-DF predicts is almost identical to the bond length obtained from a standard PBE calculation. It turns out that the nonlocal part of the functional (E_c^{nl}) only makes a negligible contribution to the total energy. In this regard, the total exchange-correlation energy computed with the vdW-DF is just the sum of the $E_x^{\text{revPBE}}[n]$ and $E_c^{\text{LDA}}[n]$, i.e. revPBE exchange and LDA correlation. It remains to be determined whether this form of exchange-correlation energy is appropriate for the system of interest, but the main point is that in the regime of weak van der Waals forces, the vdW-DF will not change or alter well established DFT results. We will readdress the question of covalently bonded systems and vdW-DF in the context of a solid in Sec. III E.

Now we turn to the bonding of the CO₂ dimer. We have performed calculations for the interaction energy of this dimer as a function of the dimer separation and slip distance. We find that the preferred parallel slip distance is 2.05 Å, and the corresponding interaction energy as a function of dimer separation is depicted in Fig. 4. Similar to Ar and Kr, the results indicate that the differences between non-SC and SC vdW-DF calculations are negligible. Furthermore, the C–C separation distance of 3.772 Å is in good agreement with the experimentally determined separation distance of 3.602 Å.³⁷ The vdW-DF interaction energy of 1.55 kcal/mol is comparable to the MP2 value of 1.36 kcal/mol (extrapolated to the complete basis set limit)³⁸ as well as the value of 1.60

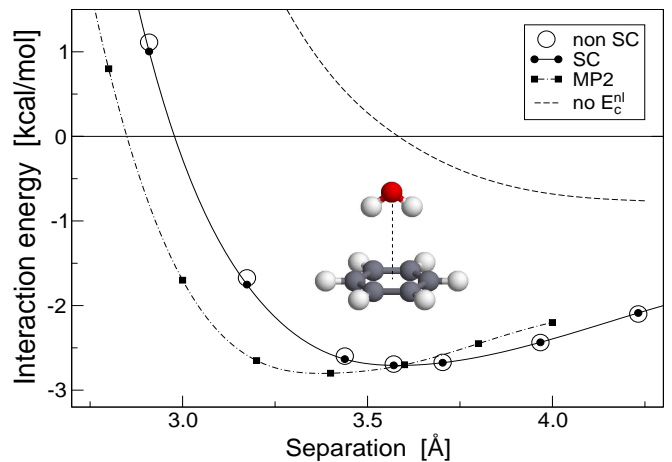


FIG. 5: Interaction energy of water on benzene. The little inset shows the geometry.

kcal/mol determined by Becke and coworkers using their density-functional model for the dispersion interaction.³⁹ In addition, Fig. 4 shows that the equilibrium separation distance for the CO₂ dimer is slightly larger than the MP2 results.³⁸

As before, by looking at the “no E_c^{nl} ” curve we can see that most of the binding originates in the nonlocal part of the functional.

C. Water on benzene

We now move to the physically and chemically more interesting question of how a typical solvent like water binds to hydrocarbons. Here, we consider the simple test case of the interaction energy between water and benzene. We limit ourselves to a particular configuration, in which the water molecule is positioned with the hydrogen atoms at equivalent heights pointing towards the benzene plane. The oxygen atom is positioned directly above the center of the benzene molecule, as depicted in the little inset in Fig. 5.

First, we relaxed the bond length of the water molecule and benzene ring individually. The optimal H–O bond length for the water molecule and the H–O–H angle were found to be 0.973 Å and 106°, respectively, in quite good agreement with the experimental values of 0.958 Å and 104.5°.⁴⁰ The C–C and C–H bond lengths for the benzene molecule were 1.396 Å and 1.100 Å, where experiments find 1.397 Å and 1.084 Å, respectively.⁴⁰ Our results for the interaction energy versus the vertical separation distance between the oxygen atom and the center of the benzene ring is plotted in Fig. 5. Again, we see that the difference between SC and non-SC calculations is very small. Consistent with our previous results, the difference is more evident at shorter separation distances. For comparison, we plotted the results from a recent MP2 study.²⁷ We find fair agreement, with MP2 calculations

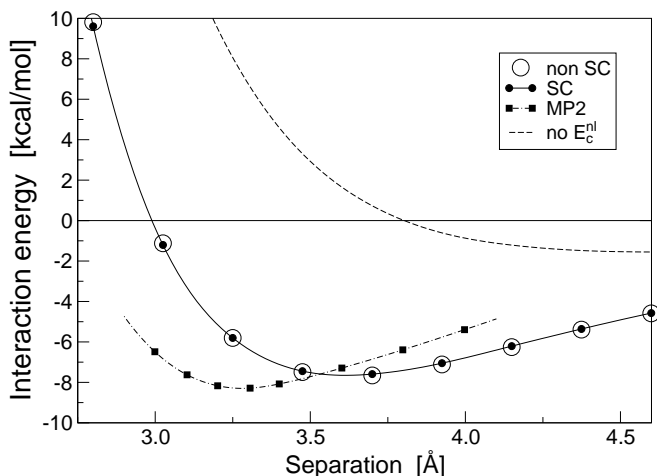


FIG. 6: Interaction energy of a cytosine dimer as a function of separation.

giving a shorter equilibrium distance and lower interaction energies than vdW-DF. The difference for both is less than 5%.

Once again, we find that without E_c^{nl} , the complex binds at a much too large distance with much weaker binding energies—supporting the fact that the nonlocal correlation energy is crucial for the correct description of van der Waals binding.

D. Cytosine dimer

The applicability of vdW-DF to monosubstituted benzene dimers has been shown in Ref. [13]. We will now extend this work by considering cytosine, a simple nucleic acid base.

We study the interaction energy of a cytosine dimer as a function of separation (Fig. 6). The geometry is such that the two molecules are placed on top of each other with one of them rotated by 180° around an axis that passes through the center of both rings. Consistent with other findings reported in this paper, there are no significant differences between the SC and non-SC results. Similarly as in the cases before, the “no E_c^{nl} ” curve reveals that the majority of the binding energy comes from the nonlocal contribution of the vdW-DF. As usual, while the comparison to MP2 calculations is quite good, we find a slightly larger binding distance.

E. Crystalline Silicon

We now choose to apply the new functional to an extended system and return to the question raised in Sec. III B. We purposefully selected an extended system in which the bonding is mostly covalent and where van der Waals interactions should be unimportant. Again,

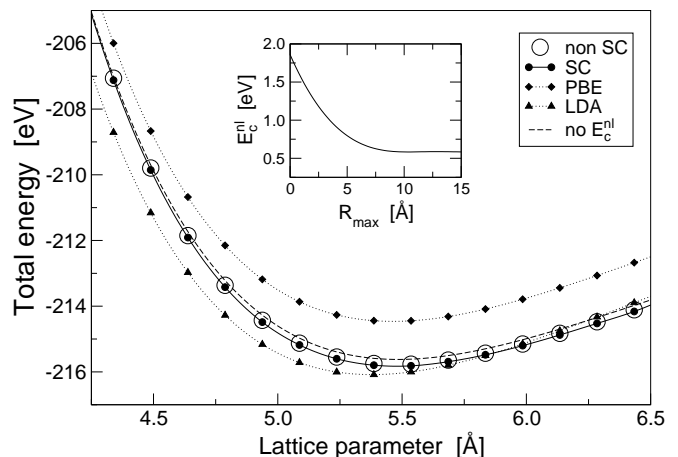


FIG. 7: Total energy (per two-atom unit cell) of Si as a function of the lattice constant. The inset shows the convergence of E_c^{nl} with respect to the cutoff radius R_{max} . See text for further details.

we seek to understand how the vdW-DF treats such systems.

In Fig. 7, we plot the total energy (per two-atom unit cell) of crystalline silicon as a function of the lattice parameter. In addition to the “usual” curves for SC and non-SC results, which show no differences, we now include results from calculations performed with standard LDA and PBE functionals. The main point of Fig. 7 is that all calculations result in very similar lattice constants: non-SC (5.48 Å), SC (5.48 Å), no E_c^{nl} (5.48 Å), PBE (5.46 Å), and LDA (5.37 Å). In other words, the nonlocal contribution in systems like silicon is indeed negligible and the functional performs as expected for the local and semilocal contributions, i.e. revPBE exchange and LDA correlation. This is even more evident in the fact that the lines for SC and “no E_c^{nl} ” almost coincide, resulting in exactly the same lattice constant.

At this point, we would also like to mention another important aspect of periodic systems. Since crystalline Si is an extended system, interactions between different unit cells have to be included when the energy in Eq. (1) and the potential in Eq. (16) are evaluated. From Fig. 1 it is apparent that all kernel functions decrease in absolute magnitude with increasing D , and in turn, also with increasing separation $|\mathbf{r} - \mathbf{r}'|$ of the two points \mathbf{r} and \mathbf{r}' . Thus, it is natural to introduce a maximum distance R_{max} above which the contribution of a given pair \mathbf{r} and \mathbf{r}' is no longer included. For the case of Si, the convergence of E_c^{nl} with respect to this cutoff radius R_{max} is depicted in the inset in Fig. 7. It can be seen that the convergence is quicker than for materials containing carbon.^{17,18} For the purpose of this study we have chosen $R_{\text{max}} = 15$ Å.

The findings for crystalline silicon parallel the earlier findings for the CO_2 molecule in Sec. III B: When the van der Waals interactions in an extended system become negligible, the contribution of the nonlocal part E_c^{nl}

to the total energy becomes negligible. Again, vdW-DF does not affect well established DFT results. With this, we conclude our quantitative results and move on to a qualitative description of the van der Waals bond.

IV. NATURE OF THE VAN DER WAALS BOND

The conventional picture of the van der Waals interaction envisions in its simplest form two fragments with distinct charge distributions, whose motions are correlated so as to reduce the interfragment electron-electron repulsion and hence produce a net attractive force between the fragments. For distant fragments the dipolar interactions caused by these correlations are dominant, and one obtains the familiar attractive r^{-6} interaction (at *very* large distances, typically 100 Å or more, this interaction is further weakened by relativistic retardation effects). The vdW-DF method embraces this picture, which indeed was central to its derivation, and also includes the contribution of more complex correlated motions that occur as the fragments get closer and even merge.

However, the van der Waals bond must also have a completely different feature as part of its nature. This feature arises because the nuclei are classical particles influenced only by Coulomb forces and immune to the fluctuations in such forces due to the more rapid electronic motions. Because of the stationary property of the energy with respect to variations in the wave function, these forces are easily calculated—a result often attributed to Hellmann⁴¹ and Feynman,⁴² but whose foundation is much older.^{43,44} The consequence is that the static or ground state electronic charge distribution must deform itself in such a way as to produce the required forces on the nuclei by classical Coulomb interactions alone. This concept is familiar for covalent bonds, but how is it implemented for van der Waals bonds?

We can now answer this question by calculating how the static charge density changes when the nonlocal contribution E_c^{nl} is included in the functional. To this end, we investigate the density of the Ar dimer in a plane that includes both atoms. We calculate the induced electron density that occurs when the atoms bond, i.e. $n_{ind} = n_{bond} - n_{atom}$, where n_{bond} is the density of the dimer and n_{atom} is the density of the isolated atoms. We can now study the difference in the induced electron density when the full functional is used n_{ind}^{full} , compared to the induced density that results without the nonlocal part $n_{ind}^{no.nl}$. Results for $n_{ind}^{full} - n_{ind}^{no.nl}$ for a separation of 4.02 Å are depicted in Fig. 8. The plot shows the change in the induced electron density when the nonlocal part of the functional is “turned on.” As expected, it can be seen that the electron density from around the nuclei moves between the atoms, which in turn explains the stronger binding in terms of implied changes in the electrostatic forces on the nuclei arising from this charge redistribution. Although the change in density is very

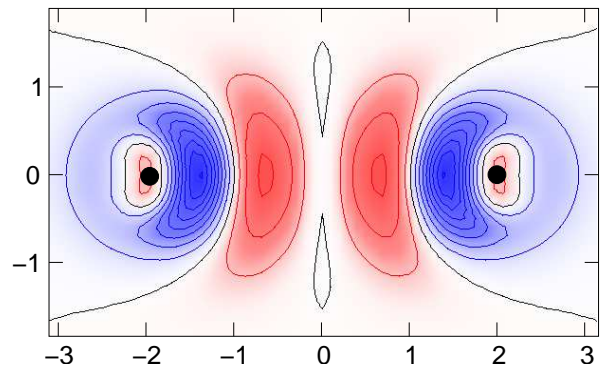


FIG. 8: The bonding charge of a van der Waals complex. Shown is the difference in induced electron density $n_{ind}^{full} - n_{ind}^{no.nl}$ for the Ar dimer with a separation of 4.02 Å. The scale is in Å and the black dots mark the position of the nuclei. The zero level is marked by the black contour. Red areas represent areas of electron density gain when the nonlocal part is included; conversely, blue areas indicate loss of electron density. Increments between contour lines are 5×10^{-5} electrons/Å³.

small ($\sim 10^{-4}$ electrons/Å³), the resulting binding energies and forces change considerably, as seen in Figs. 2 and 3. This is the van der Waals analogue of the bonding charge familiar from the theory of the covalent bond, although it is much weaker and of different shape.

V. CONCLUSIONS

The long-range part of the Kohn-Sham exchange correlation potential derived here allows the vdW-DF theory of Dion et al.¹⁰ to be applied in a fully self-consistent manner. In previous work the vdW-DF functional had been applied as a post-GGA perturbation. It was argued that this was a reasonable approximation, because one does not expect that the rather weak and diffuse vdW interaction should substantially change the electronic charge distribution. The present work, through the application of the fully self-consistent theory to a number of van der Waals complexes, shows that this argument was correct. In all the complexes studied, the predictions of the fully self-consistent theory were nearly indistinguishable from those obtained via post-GGA perturbation. This was true near the equilibrium separation between the fragments. However, inaccuracies in the perturbation method began to become noticeable when the fragments were pushed together more closely and the perturbation becomes larger. The above conclusions additionally validate the many previously performed post-GGA perturbative calculations, and suggest that the more efficient post-GGA perturbative method will remain an effective tool.

Nevertheless, the availability of a self-consistent theory is important, because it unleashes the possibility of applying a number of important and standard DFT tech-

niques whose availability depends on this self-consistency. The most obvious of these is the ability to calculate inter-nuclear forces via electrostatics. Indeed we show that the Hellmann-Feynman forces are given accurately in vdW-DF, a feature that will allow for efficient nuclear relaxation methods to be employed to determine optimal geometric structures.

Finally, our applications to the geometries of isolated molecules as well as bulk silicon suggest that vdW-DF is really a general density functional. It gives good results for systems or parts thereof where van der Waals forces are substantial, but does not spoil the results of ordinary LDA-GGA type functionals when van der Waals forces are unimportant.

These studies have shown the strengths of the existing functional. However, areas for future improvements are also important. One of these is the consistent small overestimation of the separation between vdW bound fragments. This occurs in all the vdW complexes considered here, as well as those considered in previous work.^{12,13,17,18} The reason for this persistent shift has been attributed to inadequacies of the exchange functional,^{12,13,18} but a systematic study has yet to be done. It seems likely that the source of this discrepancy can be unambiguously identified and corrected in future work.

Acknowledgments

We are grateful to Henrik Rydberg and Bengt Lundqvist, without whom there would not have been this functional, to Maxime Dion for proving its usefulness for real van der Waals complexes, and to Elsebeth Schröder, who led the development of methods for handling extended systems. This work was supported by NSF Grant No. DMR-0456937. All calculations were performed on the Rutgers high-performance supercomputer facility, operated by the Center for Materials Theory of the Department of Physics and Astronomy. PH thanks the Swedish Research Council (VR).

APPENDIX A: DETAILS OF THE EVALUATION OF THE KERNEL

The expression for the kernel ϕ can be written as¹⁰

$$\begin{aligned} \phi(d, d') &= \frac{2}{\pi^2} \int_0^\infty a^2 da \int_0^\infty b^2 db W(a, b) \\ &\times T(\nu(a), \nu(b), \nu'(a), \nu'(b)) , \end{aligned} \quad (\text{A1})$$

where the function $W(a, b)$ is defined as

$$\begin{aligned} W(a, b) &= \frac{2}{a^3 b^3} \left[\right. \\ &(3 - a^2)b \cos b \sin a + (3 - b^2)a \cos a \sin b \\ &\left. + (a^2 + b^2 - 3) \sin a \sin b - 3ab \cos a \cos b \right] , \end{aligned} \quad (\text{A2})$$

and the function T is given by

$$\begin{aligned} T(w, x, y, z) &= \frac{1}{2} \left[\frac{1}{w+x} + \frac{1}{y+z} \right] \\ &\times \left[\frac{1}{(w+y)(x+z)} + \frac{1}{(w+z)(y+x)} \right] . \end{aligned} \quad (\text{A3})$$

Furthermore, we have used the definitions

$$\nu(u) = u^2/2h(u/d) , \quad (\text{A4a})$$

$$\nu'(u) = u^2/2h(u/d') , \quad (\text{A4b})$$

and

$$h(t) = 1 - \exp(-4\pi t^2/9) . \quad (\text{A5})$$

Since ϕ according to Eq. (A1) depends on d only via ν and on d' only via ν' , it is straightforward to perform the required derivatives indicated in Eqs. (18) analytically, leaving only the double integral over a and b in Eq. (A1) to be done numerically. The required partial derivatives of $T(\nu(a), \nu(b), \nu'(a), \nu'(b))$ in Eq. (A1) are T_d , T_{dd} , and $T_{dd'}$, where ν and ν' depend implicitly on d and d' respectively according to Eqs. (A4). Thus, T_d , T_{dd} , and $T_{dd'}$ may be expressed in terms of partial derivatives of $T(w, x, y, z)$ in Eq. (A3) with respect to w, x, y, z , and the partial derivatives of ν and ν' in Eqs. (A4) with respect to d and d' . This procedure gives

$$T_d = T_w \nu_d(a) + T_x \nu_d(b) , \quad (\text{A6a})$$

$$\begin{aligned} T_{dd} &= T_{ww} \nu_d^2(a) + T_{ww} \nu_{dd}(a) + T_{xx} \nu_d^2(b) \\ &+ T_{xx} \nu_{dd}(b) + 2T_{wx} \nu_d(a) \nu_d(b) , \end{aligned} \quad (\text{A6b})$$

$$\begin{aligned} T_{dd'} &= T_{wy} \nu'_{d'}(a) \nu_d(a) + T_{wz} \nu'_{d'}(b) \nu_d(a) \\ &+ T_{xy} \nu'_{d'}(a) \nu_d(b) + T_{xz} \nu'_{d'}(b) \nu_d(b) . \end{aligned} \quad (\text{A6c})$$

The algebraic evaluation of the derivatives in Eqs. (A6) is most simply done with a symbolic algebra program. Then, altering Eq. (A1) by the replacement of T with dT_d using Eq. (A6a) gives Φ_1 (Eq. (18a)). An analogous replacement using $d^2 T_{dd}$ gives Φ_2 (Eq. (18b)), while for Φ_3 (Eq. (18c)) the replacement should be made with $T_d + dT_{dd} + d'T_{dd'}$.

APPENDIX B: GRADIENT CORRECTION

As discussed in Ref. [10], the long range part of the correlation energy E_c^{nl} is calculated assuming a simple single pole model for the necessary response function, with parameters determined by sum rules plus the requirement that the correct energy density should be obtained when it is applied locally, i.e., according to LDA with the appropriate gradient correction. In particular, the gradient terms that represent an (inappropriate) attempt to expand the van der Waals interaction in a gradient series should be omitted.

The leading gradient contribution to the exchange-correlation energy density may be written as

$$\varepsilon_{\text{grad}} = Z \frac{e^2 k_F}{12\pi} \left(\frac{\nabla n}{2k_F n} \right)^2. \quad (\text{B1})$$

This defines the quantity Z according to the usage of Langreth and Perdew^{45,46} and Langreth and Vosko.⁴⁷ Rasolt and Geldart^{48,49} define a Z which is larger by an additive constant of $4/3$, which would cause a corresponding change in Eq. (B1). The sometimes confusing aspects of this notation have been clarified more recently.⁵⁰ The value of Z was first inferred by combining the calculations of Ma and Brueckner⁵¹ and Sham,⁵² giving the result $Z = 1.1978$. The positive sign was unexpected, and gave a correction to the LDA that went in the wrong direction, setting back the application of gradient corrections for years.

The first step in the resolution of this puzzle came with Rasolt and Geldart's breakdown of Z according to the process involved, dividing $Z = Z_{ab} + Z_c$, according to the processes depicted in Fig. 1a,b,c of Ref. [48] and Fig. 3a,b,c of Ref. [49], and also Fig. 4a,b,c of Ref. [46] where the same results were obtained by a different method. The inset c in each of these figures shows what is known as the fluctuation diagram. It is the cause of the unphysical positive contribution to Z : one finds $Z_{ab} = -0.8491$ and $Z_c = 2.0470$.

It would be another decade, however, before the implications of the fluctuation diagram would become fully apparent. This began with a seminal paper by Maggs and Ashcroft,⁵³ who showed that the diagram was associated with the van der Waals interaction, followed by further development,^{47,54} and culminating⁵⁵ with the use of the fluctuation diagram to obtain the London formula for the van der Waals interaction between two atoms. The reason for the failure of the gradient expansion was now apparent: the calculation of Z_c represented an attempt to expand the long-range vdW interaction in powers of density gradients, an enterprise that was in retrospect obviously doomed to fail.

Based on these facts, we write for use as the second term on the right side of Eq. (12) of Ref. [10]

$$\varepsilon_{\text{grad}} = Z_{ab} \frac{e^2 k_F}{12\pi} \left(\frac{\nabla n}{2k_F n} \right)^2. \quad (\text{B2})$$

The van der Waals contribution is already included in another way, and it would be double counting to add the gradient expansion to it in addition. This is a matter of principle, but convenient indeed, because it avoids the use of Z_c , which fails to be a valid approximation. This explains the use of Z_{ab} rather than Z in Eq. (7).

In principle, Z_{ab} is not a constant, but rather a function of electronic density. There is no published data on this dependence. In Fig. 2 of Ref. [45] are shown two calculations that give the density dependence of the full Z , one of which was obtained earlier^{48,49} [Z is equal to the ordinate of that figure times a numerical constant]. When the calculations of Ref. [45] were made, the density dependence of Z_{ab} and Z_c were calculated separately, but the significance of the individual quantities was not known at that time, and individual results were not presented. However, the common author of this paper and Ref. [45], who did this part of the calculation, attests that the principal density dependence shown in the Fig. 2 of this reference comes from that of Z_c , and that the density dependence of Z_{ab} was weak. We thus feel comfortable using the high density value of $Z_{ab} = -0.8491$.

APPENDIX C: EVALUATION OF THE GRADIENT

In the following, we will focus on the term $\nabla \cdot [\dots]$ in Eq. (15). It is straight forward to see that

$$\begin{aligned} \nabla \cdot \left[\phi_d(\mathbf{r}, \mathbf{r}') R_{\mathbf{r}\mathbf{r}'} \mathbf{s}(\mathbf{r}) \right] &= (\nabla \phi_d(\mathbf{r}, \mathbf{r}')) R_{\mathbf{r}\mathbf{r}'} \cdot \mathbf{s}(\mathbf{r}) + \\ &+ \phi_d(\mathbf{r}, \mathbf{r}') (\nabla R_{\mathbf{r}\mathbf{r}'} \cdot \mathbf{s}(\mathbf{r}) + \phi_d(\mathbf{r}, \mathbf{r}') R_{\mathbf{r}\mathbf{r}'} \nabla \cdot \mathbf{s}(\mathbf{r})). \end{aligned}$$

The gradient of $R_{\mathbf{r}\mathbf{r}'}$ is the unit vector $\hat{\mathbf{R}}_{\mathbf{r}\mathbf{r}'}$. For the gradient of $\phi_d(\mathbf{r}, \mathbf{r}')$ we abbreviate higher derivatives of $\phi(d, d')$ in the same fashion as above,

$$\frac{\partial^2 \phi(d, d')}{\partial d \partial d} = \phi_{dd}(d, d') \quad \text{and} \quad \frac{\partial^2 \phi(d, d')}{\partial d \partial d'} = \phi_{dd'}(d, d').$$

Inserting the definition of $d(\mathbf{r}, \mathbf{r}')$ and $d'(\mathbf{r}, \mathbf{r}')$ from Eq. (6), the gradient of $\phi_d(\mathbf{r}, \mathbf{r}')$ can then be written as

$$\begin{aligned} \nabla \phi_d(\mathbf{r}, \mathbf{r}') &= \phi_{dd}(\mathbf{r}, \mathbf{r}') \nabla d(\mathbf{r}, \mathbf{r}') + \phi_{dd'}(\mathbf{r}, \mathbf{r}') \nabla d'(\mathbf{r}, \mathbf{r}') \\ &= \phi_{dd}(\mathbf{r}, \mathbf{r}') (\hat{\mathbf{R}}_{\mathbf{r}\mathbf{r}'} q_0(\mathbf{r}) + R_{\mathbf{r}\mathbf{r}'} \nabla q_0(\mathbf{r})) \\ &+ \phi_{dd'}(\mathbf{r}, \mathbf{r}') \hat{\mathbf{R}}_{\mathbf{r}\mathbf{r}'} q_0(\mathbf{r}'). \end{aligned} \quad (\text{C1})$$

If we collect corresponding terms, the complete gradient in Eq. (15) is then easily seen to be

$$\begin{aligned} \nabla \cdot \left[\phi_d(\mathbf{r}, \mathbf{r}') R_{\mathbf{r}\mathbf{r}'} \mathbf{s}(\mathbf{r}) \right] &= \hat{\mathbf{R}}_{\mathbf{r}\mathbf{r}'} \cdot \mathbf{s}(\mathbf{r}) \times \\ &\left[\phi_d(\mathbf{r}, \mathbf{r}') + \phi_{dd}(\mathbf{r}, \mathbf{r}') q_0(\mathbf{r}) R_{\mathbf{r}\mathbf{r}'} + \phi_{dd'}(\mathbf{r}, \mathbf{r}') q_0(\mathbf{r}') R_{\mathbf{r}\mathbf{r}'} \right] \\ &+ \phi_{dd}(\mathbf{r}, \mathbf{r}') R_{\mathbf{r}\mathbf{r}'}^2 \mathbf{s}(\mathbf{r}) \cdot \nabla q_0(\mathbf{r}) + \phi_d(\mathbf{r}, \mathbf{r}') R_{\mathbf{r}\mathbf{r}'} \nabla \cdot \mathbf{s}(\mathbf{r}). \end{aligned}$$

Expression for $\phi_d(d, d')$, $\phi_{dd}(d, d')$, and $\phi_{dd'}(d, d')$ are discussed in Appendix A.

¹ J. P. Perdew, J. A. Chevary, S. H. Vosko, K. A. Jackson, M. R. Pederson, D. J. Singh, and C. Fiolhais, Phys. Rev.

B **46**, 6671 (1992); Erratum: **48**, 4978 (1993).
² J. P. Perdew, K. Burke, and M. Ernzerhof, Phys. Rev.

- Lett. **77**, 3865 (1996).
- ³ Y. Zhang and W. Yang, Phys. Rev. Lett. **80**, 890 (1998).
 - ⁴ V. N. Staroverov, G. E. Scuseria, J. Tao, and J. P. Perdew, J. Chem. Phys. **119**, 12129 (2003).
 - ⁵ V. N. Staroverov, G. E. Scuseria, J. Tao, and J. P. Perdew, Phys. Rev. B **69**, 75102 (2004).
 - ⁶ J. Šponer, J. Leszczynski, and P. Hobza, J. Comput. Chem. **17**, 841 (1996); P. Hobza, J. Šponer, and T. Reschel, J. Comput. Chem. **16**, 1315 (1995).
 - ⁷ S. Kristyan and P. Pulay, Chem. Phys. Lett. **229**, 175 (1994).
 - ⁸ E. Ruiz, D. R. Salahub, A. Vela, J. Am. Chem. Soc. **117**, 1141 (1995).
 - ⁹ H. Rydberg, M. Dion, N. Jacobson, E. Schröder, P. Hyldgaard, S. I. Simak, D. C. Langreth, and B. I. Lundqvist, Phys. Rev. Lett. **91**, 126402 (2003).
 - ¹⁰ M. Dion, H. Rydberg, E. Schröder, D. C. Langreth, and B. I. Lundqvist, Phys. Rev. Lett. **92**, 246401 (2004); *ibid.* **95**, 109902 (2005).
 - ¹¹ D. C. Langreth, M. Dion, H. Rydberg, E. Schröder, P. Hyldgaard, and B. I. Lundqvist, Int. J. Quantum Chem. **101**, 599 (2005).
 - ¹² A. Puzder, M. Dion, and D. C. Langreth, J. Chem. Phys. **124**, 164105 (2006).
 - ¹³ T. Thonhauser, A. Puzder, and D. C. Langreth, J. Chem. Phys. **124**, 164106 (2006).
 - ¹⁴ S. D. Chakarova-Käck, J. Kleis, and E. Schröder, *Dimers of polycyclic aromatic hydrocarbons in density functional theory*, Applied Physics Report 2005-16; this work supercedes an earlier method (Ref. [15]) for extracting finite dimer energies from an infinite double layer.
 - ¹⁵ S. D. Chakarova and E. Schröder, J. Chem. Phys. **122**, 54102 (2005).
 - ¹⁶ S. Tsuzuki, K. Honda, T. Uchimaru, and M. Mikami, J. Chem. Phys. **120**, 647 (2004).
 - ¹⁷ S. D. Chakarova-Käck, E. Schröder, B. I. Lundqvist, and D. C. Langreth, Phys. Rev. Lett. **96**, 146107 (2006).
 - ¹⁸ J. Kleis, B. I. Lundqvist, D. C. Langreth, and E. Schröder, cond-mat/0611498 (unpublished).
 - ¹⁹ C. Møller and M. S. Plesset, Phys. Rev. **46**, 618 (1934); M. Head-Gordon, J. A. Pople, and M. J. Frisch, Chem. Phys. Lett. **153**, 503 (1988).
 - ²⁰ J. Čížek, J. Chem. Phys. **45**, 4256 (1966); Adv. Chem. Phys. **14**, 35 (1969); J. A. Pople, M. Head-Gordon, and K. Raghavachari, J. Chem. Phys. **87**, 5968 (1987), and Refs. 8–15 therein.
 - ²¹ E. Ziambaras, J. Kleis, E. Schröder, and P. Hyldgaard, “Potassium intercalation in graphite: A van der Waals density-functional study” (unpublished).
 - ²² M. Elstner, P. Hobza, T. Frauenheim, S. Suhai, and E. Kaxiras, J. Chem. Phys. **114**, 5149 (2001).
 - ²³ X. Wu, M. C. Vargas, S. Nayak, V. Lotrich, and G. Scoles, J. Chem. Phys. **115**, 8748 (2001).
 - ²⁴ Q. Wu and W. Yang, J. Chem. Phys. **116**, 515 (2002).
 - ²⁵ M. Hasegawa and K. Nishidate, Phys. Rev. B **70**, 205431 (2004).
 - ²⁶ S. Grimme, J. Comput. Chem. **25**, 1463 (2004).
 - ²⁷ U. Zimmerli, M. Parrinello, and P. Koumoutsakos, J. Chem. Phys. **120**, 2693 (2004).
 - ²⁸ M. Elstner, D. Porezag, G. Jungnickel, J. Elsner, M. Haugk, T. Frauenheim, S. Suhai, and G. Seifert, Phys. Rev. B **58**, 7260 (1998).
 - ²⁹ D. Sanches-Portal, P. Ordejon, E. Artacho, and J. M. Soler, Int. J. Quantum Chem. **65**, 453 (1997).
 - ³⁰ John P. Perdew and Y. Wang, Phys. Rev. B **33**, 8800 (1986).
 - ³¹ John P. Perdew and Y. Wang, Phys. Rev. B **45**, 13244 (1992).
 - ³² Y. U. Barash, Fiz. Tverd. Tela (Leningrad) **30**, 1578 (1988) [Sov. Phys. Solid State **30**, 1580 (1988)].
 - ³³ Y. U. Barash and O. I. Notysh, Zh. Eksp. Teor. Fiz. **98**, 542 (1990) [Sov. Phys. JETP **71**, 301 (1990)]; B. E. Sernelius and P. Björk, Phys. Rev. B **57**, 6592 (1998); M. Boström and B. E. Sernelius, Phys. Rev. B **61**, 2204 (2000); J. F. Dobson, A. White, and A. Rubio, Phys. Rev. Lett. **96**, 073201 (2006).
 - ³⁴ X. Gonze *et al.*, Comp. Mat. Sci. **25**, 478 (2002).
 - ³⁵ J. R. Chelikowsky, N. Troullier, and Y. Saad, Phys. Rev. Lett. **72**, 1240 (1994); J. R. Chelikowsky, J. of Phys. D **33**, R33 (2000); M. M. G. Alemany, M. Jain, L. Kronik, and J. R. Chelikowsky, Phys. Rev. B **69**, 075101 (2004).
 - ³⁶ J. Ogilvie and F. Wang, J. Mol. Struct. **273**, 277 (1992).
 - ³⁷ M. A. Walsh, T. H. England, T. R. Dyke, and B. J. Howard, Chem. Phys. Lett. **142**, 265 (1987).
 - ³⁸ S. Tsuzuki, T. Uchimaru, M. Mikami, and K. Tanabe, J. Chem. Phys. **109**, 2169 (1998).
 - ³⁹ A. D. Becke and E. R. Johnson, J. Chem. Phys. **123**, 154101 (2005).
 - ⁴⁰ *NIST Chemistry Webbook, NIST Standard Reference Database*, edited by P. J. Linstrom and W. G. Mallard (National Institute of Standards and Technology, Gaithersburg, MD, 2001), Number 69 (<http://webbook.nist.gov>).
 - ⁴¹ H. Hellmann, *Einführung in die Quantenchemie* (Franz Deutsche, Leipzig, 1937).
 - ⁴² R. P. Feynman, Phys. Rev. **56**, 340 (1939).
 - ⁴³ P. Ehrenfest, Z. Phys. **45**, 455 (1927).
 - ⁴⁴ W. Pauli, *Handbuch der Physik* (Springer, Berlin, 1933).
 - ⁴⁵ D. C. Langreth and J. P. Perdew, Solid State Commun. **31**, 567 (1979).
 - ⁴⁶ D. C. Langreth and J. P. Perdew, Phys. Rev. B **21**, 5469 (1980).
 - ⁴⁷ D. C. Langreth and S. H. Vosko, Phys. Rev. Lett. **59**, 497 (1987).
 - ⁴⁸ M. Rasolt and D. J. W. Geldart, Phys. Rev. Lett. **35**, 1234, (1975).
 - ⁴⁹ D. J. W. Geldart and M. Rasolt, Phys. Rev. B **13**, 1477 (1976).
 - ⁵⁰ D. C. Langreth and S. H. Vosko, Adv. Quantum Chem. **21**, 175 (1990).
 - ⁵¹ S.-K. Ma and K. Brueckner, Phys. Rev. **165**, 18 (1968).
 - ⁵² L. J. Sham in *Computational Methods in Band Theory*, edited by P. M. Marcus, J. F. Janak, and A. R. Williams (Plenum, New York, 1971), p. 458.
 - ⁵³ A. C. Maggs and N. W. Ashcroft, Phys. Rev. Lett. **59**, 113 (1987).
 - ⁵⁴ K. Rapcewicz and N. W. Ashcroft, Phys. Rev. B **44**, 4032 (1991).
 - ⁵⁵ Y. Andersson, D. C. Langreth, and B. I. Lundqvist, Phys. Rev. Lett. **76**, 102 (1996).